Diabetologia (2001) 44: 2171–2179

Diabetologia

Human adipose tissue glucose uptake determined using [^{18}F]-fluoro-deoxy-glucose ([^{18}F]FDG) and PET in combination with microdialysis

K. A. Virtanen[1], P. Peltoniemi[1], P. Marjamäki[1], M. Asola[2], L. Strindberg[3], R. Parkkola[5], R. Huupponen[4], J. Knuuti[1], P. Lönnroth[3], P. Nuutila[1, 2]

[1] Turku PET Centre, University of Turku, Turku, Finland
[2] Department of Internal Medicine, Turku University Central Hospital, Turku, Finland
[3] Department of Internal Medicine, University of Gothenburg, Gothenburg, Sweden
[4] Department of Pharmacology and Clinical Pharmacology, University of Turku, Turku, Finland
[5] Department of Radiology, Turku University Central Hospital, Turku, Finland

Abstract

Aims/hypothesis. To determine the lumped constant (LC), which accounts for the differences in the transport and phosphorylation between [^{18}F]-2-fluoro-2-deoxy-D-glucose ([^{18}F]FDG) and glucose, for [^{18}F]FDG in human adipose tissue.
Methods. [^{18}F]FDG-PET was combined with microdialysis. Seven non-obese (29 ± 2 years of age, BMI 24 ± 1 kg/m^2) and seven obese (age 32 ± 2 years of age, BMI 31 ± 1 kg/m^2) men were studied during euglycaemic hyperinsulinaemia (1 mU/kg · min^{-1} for 130 min). Abdominal adipose tissue [^{18}F]FDG uptake (rGU_{FDG}) and femoral muscle glucose uptake were measured using [^{18}F]FDG-PET. Adipose tissue perfusion was measured using [^{15}O]-labelled water and PET, and interstitial glucose concentration using microdialysis. Glucose uptake (by microdialysis, rGU_{MD}) was calculated by multiplying glucose extraction by regional blood flow. The LC was determined as the ratio of rGU_{FDG} to rGU_{MD}.
Results. Rates of adipose tissue glucose uptake (rGU_{MD}) were 36% higher in the non-obese than in the obese patients (11.8 ± 1.7 vs 7.6 ± 0.8 μmol/kg · min^{-1}, $p < 0.05$, respectively) and a correlation between rGU_{MD} and rGU_{FDG} was found ($r = 0.82$, $p < 0.01$). The LC averaged 1.14 ± 0.11, being similar in the obese and the non-obese subjects (1.01 ± 0.15 vs 1.26 ± 0.15, respectively, NS). Muscle glucose uptake was fourfold to fivefold higher than adipose tissue glucose uptake in both groups.
Conclusion/interpretation. [^{18}F]FDG-PET seems a feasible tool to investigate adipose tissue glucose metabolism in human beings. Direct measurements with [^{18}F]FDG-PET and microdialysis suggest a LC value of 1.14 for [^{18}F]FDG in human adipose tissue during insulin stimulation and the LC does not appear to be altered in insulin resistance. Furthermore, the obese patients show insulin resistance in both adipose tissue and skeletal muscle. [Diabetologia (2001) 44: 2171–2179]

Keywords Adipose tissue, glucose, insulin, [^{18}F]FDG, PET, microdialysis, skeletal muscle, obesity.

Received: 10 May 2001 and in revised form: 29 August 2001

Corresponding author: P. Nuutila, Turku PET Centre, University of Turku, P. O. Box 52, 20521 Turku, Finland
e-mail: pirjo.nuutila@utu.fi
Abbreviations: [^{18}F]FDG, [^{18}F]-2-Fluoro-2-deoxy-D-glucose; PET, positron emission tomography; LC, lumped constant; rGU_{FDG}, regional glucose uptake measured with [^{18}F]FDG; rGU_{MD}, regional glucose uptake measured with microdialysis; A-V-technique, arterio-venous-technique; PS, permeability surface area product; K_i, rate of tracer uptake and phosphorylation; [^{15}O]H_2O, [^{15}O]-water; $t_{1/2}$, half-life; MRI, magnetic resonance imaging; ROI, region of interest; $[Glc]_p$, plasma glucose concentration

Adipose tissue is an active compartment of lipid and glucose metabolism in human beings. An association between both visceral [1–3] and subcutaneous [4–6] adipose tissue and insulin resistance has been reported. Methods available to study directly adipose tissue metabolism in vivo are limited in human beings and the investigation of metabolism in adipose tissue has been carried out mainly by indirect measurements in the whole body or in cannulated limbs. In recent years, the abdominal A-V-technique [7] and microdialysis [8, 9] have also enabled direct investigation of adipose tissue metabolism in vivo in human beings.

Microdialysis allows the measurement of interstitial concentrations of various substances in human adipose tissue [8] and after calibrated assessment of interstitial fluid substrate concentration, metabolic uptake can be calculated using Fick's equation [10–12]. This requires knowledge of regional blood flow and permeability surface area product (PS). In previous studies, adipose tissue blood flow has been measured using ^{133}Xenon [10, 11] or ethanol [13, 14] washout techniques, which allow only indirect and semiquantitative measurements of local tissue blood flow [15].

Studies in our laboratory [12] showed that combining microdialysis with radiowater and positron emission tomography (PET) are useful for measuring local metabolic uptake rates in vivo in human skeletal muscle. Use of radiowater and PET allows direct and regional assessment of blood flow without invasive catheterizations. In that study [12], we found a close correlation between glucose uptake measured with microdialysis and glucose uptake assessed with [^{18}F]FDG-PET suggesting that these two methods can be reliably combined.

Quantitative [^{18}F]FDG-PET methods have been widely applied to assess glucose utilisation in brain [16], heart [17, 18] and skeletal muscle [18, 19]. However, there are no previous studies measuring adipose tissue glucose uptake using [^{18}F]FDG-PET. The [^{18}F]FDG is a labelled glucose analogue in which the hydrogen in the 2-position is replaced by [^{18}F]. Glucose and [^{18}F]FDG are structurally more similar than glucose and either hydrogen or carboxyl labelled deoxyglucoses. Intracellularly, [^{18}F]FDG is phosphorylated by hexokinase and trapped in the tissue [20]. Thus, [^{18}F]FDG appears to be an ideal glucose tracer for PET studies in human myocardium and skeletal muscle [18, 19]. The fractional rate of tracer uptake and (Ki) can be calculated by using graphical analysis of plasma and tissue time activity curves [21]. Thereafter, the rate of glucose uptake can be calculated by multiplying Ki by the plasma glucose concentration then dividing this by the lumped constant (LC). LC is a correction factor, which accounts for any differences in transport and phosphorylation between [^{18}F]FDG and glucose. Recently, direct measurements using [^{18}F]FDG-PET and microdialysis suggested an LC value of 1.2 for [^{18}F]FDG in human skeletal muscle during insulin stimulation [12]. However, due to differences in metabolism between adipose tissue and skeletal muscle, this value cannot be directly converted for the quantitation of adipose tissue glucose uptake using [^{18}F]FDG-PET.

This study was undertaken to estimate the LC for [^{18}F]FDG directly in human subcutaneous adipose tissue during insulin stimulation by using two independent techniques; [^{18}F]FDG-PET and microdialysis. Our other aim was to test whether the LC is altered in insulin-resistant obese subjects and to determine whether insulin-stimulated glucose uptake is altered in subcutaneous adipose tissue in insulin-resistant obese patients compared with non-obese subjects. Furthermore, we aimed to compare glucose uptake in adipose tissue and skeletal muscle in the same subjects.

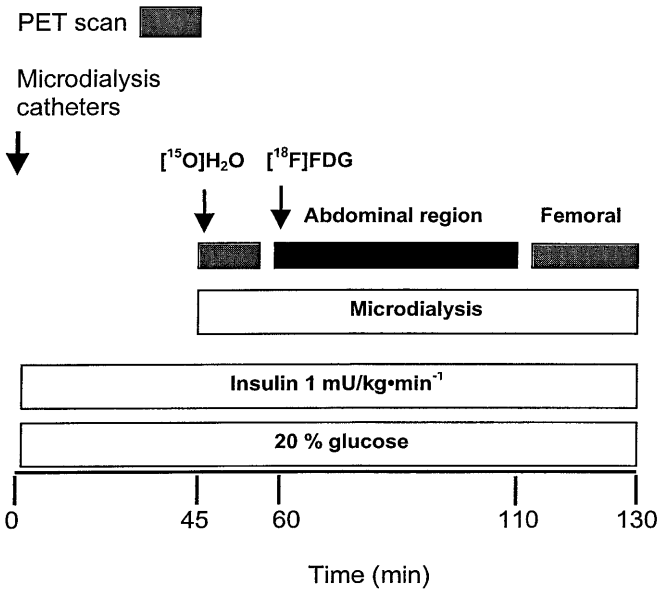

Fig. 1. Study design. Black arrows indicate the time of the microdialysis catheter insertion, and positron emitting tracer ([^{15}O]H_2O and [^{18}F]FDG) injections. Shaded rectangles denote the time period of dynamic scanning

Subject and methods

Subjects. Seven obese (32 ± 2 years of age, BMI 28–35 kg/m^2, waist-to-hip ratio, (WHR) > 1.0) and seven non-obese (age 29 ± 2 years, BMI 19–24 kg/m^2, WHR < 1.0) men were studied, their characteristics being shown in Table 1. The subjects were healthy as assessed by history, physical examination and routine laboratory tests; they were also not taking any medications. The nature, purpose and potential risks of the study were explained to all subjects before they gave their written informed consent. The Joint Commission of Ethics of the University of Turku and Turku University Central Hospital approved the study.

Study design. The study design involved studies done after an overnight fast (Fig. 1). Caffeine and nicotine had been prohibited 24 h before the study. Alcohol consumption and the consumption of meals with a fat content were avoided for 3 days and strenuous physical activity was not allowed for 48 h before the study. Two catheters were inserted. One catheter was located in a left antecubital vein for infusion of glucose and insulin, and injections of [^{15}O]H_2O and [^{18}F]FDG. Another catheter was inserted into the radial artery in the right hand for blood sampling. Each study consisted of a 130-min euglycaemic hyperinsulinaemic (1 mU/kg · min^{-1}) period. Forty-five minutes after the start of the clamp, blood flow was measured in the abdominal region using [^{15}O]H_2O. Thereafter, at 60 min [^{18}F]FDG was injected and abdominal scanning was started si-

multaneously to measure adipose tissue [^{18}F]FDG uptake. The abdominal area was scanned for 50 minutes and then the femoral region was scanned for 20 min. Microdialysis samples were collected during the [^{18}F]FDG scanning. Blood pressure and heart rate were determined basally and every 30 min throughout the study by means of an automatic oscillometric blood pressure analyser (model HEM-705C, Omron, Tokyo, Japan). Blood samples to measure radioactivity, serum insulin and plasma glucose concentrations were taken as detailed below.

Microdialysis. The microdialysis was done as previously described [23]. Commercially available custom made microdialysis catheters (20 kDa mol mass cut-off, dialysis membrane 16 · 0.5 mm; CMA, Stockholm, Sweden) were first perfused with normal saline at an infusion rate of 4.0 μl/min to wash out glycerol using a high-precision syringe pump (CMA/100 Microinjection Pump, CMA, Stockholm, Sweden). Two catheters were inserted into abdominal subcutaneous adipose tissue about 5 cm laterally to the navel, through the disinfected skin at a 45-degree angle using 18-gauge intravenous plastic cannulas. The steel mandrin was removed and the catheter placed into the tissue. The inlets of the catheters were connected to a microinjection pump (CMA/100 Microinjection Pump, CMA, Stockholm, Sweden) and perfused at a flow rate of 2.5 μl/min with saline (0.9 % NaCl). Catheters were stabilised for 30 min before changing the perfusion solution. Perfusion solution consisted of isotonic saline with the addition of 20 μmol/l glycerol, 2.5 mmol/l glucose, and 0.2 mmol/l lactate to prevent depletion of tissue nutrients [8]. After 15 min of perfusion, the first 10-min dialysate sample (pre-sample) was collected. Thereafter samples were collected at 5-min intervals for the first 20 min after [^{18}F]FDG-bolus injection and at 10-min intervals for the remaining 50 min. The relative recovery over the membrane in the microdialysis probes was determined using internal reference calibration [23]. For internal reference calibration 5 μCi/ml 3-[^{3}H]-glucose (Amersham, Buckinghamshire, UK) was added to the perfusates, and the percentage loss over the membrane was taken as an estimate of recovery. The mean in vivo recovery for glucose was 18 ± 1 % without any group differences.

Production of PET tracers. Production of [^{15}O] ($t_{1/2}$ = 123 s) was accomplished with a low-energy deuteron accelerator Cyclone 3 (Ion Beam Application, Louvain la-Neuve, Belgium). The [^{15}O]H_2O was produced using a dialysis technique in a continuously working water module [24]. An online radioactivity recording of infusions was done for each examination with a low voltage ionisation chamber [25]. Sterility and pyrogenity tests were done daily to verify the purity of the product. The [^{18}F]FDG ($t_{1/2}$ = 109 min) was synthesised with an automatic apparatus by a modified method of Hamacher et al. [26]. The specific radioactivity at the end of the synthesis was more than 75 GBq/μmol and the radiochemical purity exceeded 98 %.

Image acquisition and processing. The subjects were positioned supine in a 15-slice ECAT 931/08-tomograph (Siemens/CTI, Knoxville, Tenn, USA). Technical in-plane resolution was 6.5 mm and axial resolution was 6.7 mm in the scanner. The subject was positioned in the tomograph with the abdominal or femoral region within the gantry. Before the emission scan, a transmission scan for correction of photon attenuation was done for 5 min in both abdominal and femoral regions with a removable ring source containing [^{68}Ge]. All data were corrected for dead-time, decay and measured photon attenuation and reconstructed in a 128 · 128 matrix. For image processing, a recently developed Bayesian iterative reconstruction algorithm using median root before the 150 iterations and the Bayesian coefficient of 0.3 was applied [27]. The PET counts were converted to radioactivity concentration values (Bq/ml) using a calibration factor derived from phantom studies.

Magnetic resonance imaging (MRI). The abdominal region was imaged with a 0.23 T Outlook GP (Marconi Medical Systems, Cleveland, Ohio, USA) magnetic resonance imager using a body coil. Transverse T1-weighted field echo images with TR (Time Repetition) of 124 ms and TE (Time Echo) of 5 ms were obtained with the same pixel size as the PET images. The level of the mid-slice and the upper and lower border of the area imaged was drawn on the skin of the subjects and the same imaging area was used in PET imaging to confirm congruent data between PET and MRI. On T1-weighted MR images the adipose tissue is recognised as white, skeletal muscle as grey, water as dark grey, and bones and fast blood flow in vessels as black.

Regions of interest. MR images were fitted to the PET images. The regions of interest (ROIs) were drawn into MR images in the subcutaneous adipose tissue in the same region where microdialysis probes were located. The ROIs were copied into the flow and the [^{18}F]FDG images to cross-sectional slices from identical regions. Examples of a non-obese and an obese subject and the ROIs are presented in Figure 2. In the femoral region, ROIs were drawn in the anteromedial muscle compartments in four cross-sectional slices, carefully avoiding large blood vessels [18]. Localisation of the muscle compartments was verified by comparing the [^{18}F]FDG images with the transmission image, which provides a topographical distribution of tissue density.

Measurement of adipose tissue blood flow. For measurement of adipose tissue flow, 1.2–1.3 GBq [^{15}O]H_2O was injected intravenously and dynamic scanning was carried out for 6 minutes (6 · 5 s, 6 · 15 s, 8 · 30 s frames). To determine the input function, blood from the radial artery was continuously withdrawn using a pump at a speed of 6 ml/min. The radioactivity concentration was measured using a two-channel detector system (Scanditronix, Uppsala, Sweden) calibrated to the well counter (Wizard 1480; Wallac, Turku, Finland) and the PET scanner, as previously described [28]. The arterial input curve was corrected for dispersion and delay, as previously described [29]. The autoradiographic method, a 250-s integration time and partition value of 0.19 for adipose tissue, was applied to calculate blood flow pixel by pixel. The partition value for adipose tissue was calculated as the ratio of water content in adipose tissue to water content in blood [30].

Measurement of adipose tissue glucose uptake with [^{18}F]FDG (rGU_{FDG}). For the measurement of [^{18}F]FDG uptake 0.18–0.19 GBq of [^{18}F]FDG was injected intravenously over 60 s and a 50 min dynamic scan was simultaneously started (2 · 30 s, 4 · 60 s, 9 · 300 s frames). Arterial blood samples for the measurement of plasma radioactivity were continuously drawn and measured with the well counter as previously described [18]. The three-compartment model of [^{18}F]FDG kinetics was used as described earlier [18]. Plasma and tissue time-activity curves for the subcutaneous adipose tissue compartment on the left side of the abdomen was analysed graphically to determine the fractional rate of tracer uptake K_i [21]. Linear regression was used to determine the slope of the time-activity points between min 10 and 40 after [^{18}F]FDG injection. The rate of regional glucose uptake measured using [^{18}F]FDG (rGU_{FDG}) was calculated by multiplying fractional [^{18}F]FDG uptake (K_i) by plasma glucose concentration $[Glc]_p$.

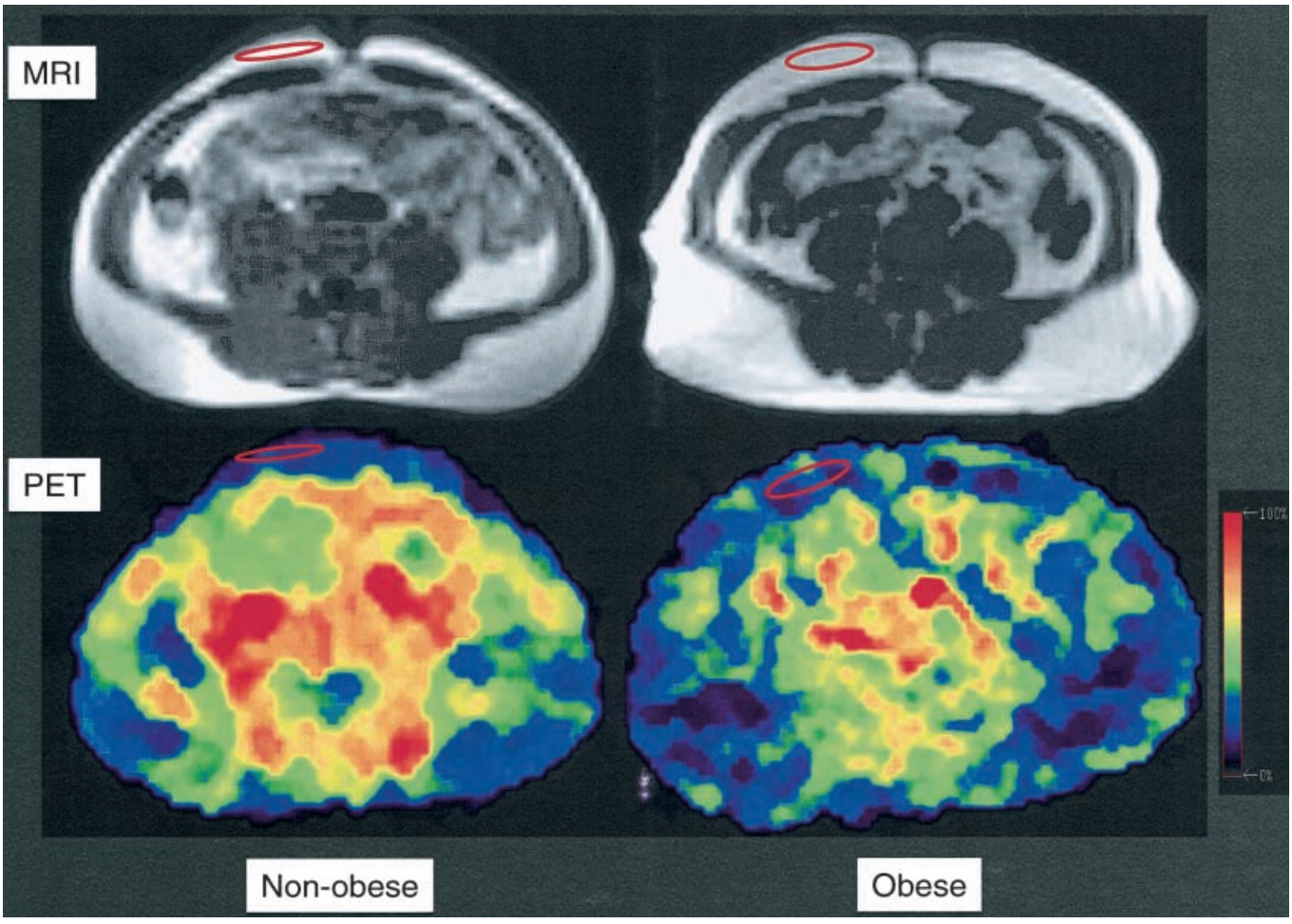

Fig. 2. An example of MRI and [^{18}F]FDG PET images from the abdominal region of a non-obese (left) and an obese subject (right). In the upper panel regions of interest (ROIs) are outlined in MR images with red colour and further copied to PET images in the same plane. In the lower panel are the PET images where the highest activity is shown in red as an index of trapping

Measurement of adipose tissue glucose uptake with microdialysis (rGU_{MD}). After calibration, interstitial glucose concentration was determined using microdialysis. Glucose uptake was calculated using Fick's equation by multiplying glucose extraction fraction with blood flow [10, 31]. Flow was measured using [^{15}O]H_2O and PET in the same adipose tissue compartment where the interstitial glucose concentration was measured, i.e., in the vicinity of the microdialysis probe. The extraction fraction for glucose was calculated as previously described [10, 31] using the glucose permeability surface area product (PS) 2 ml/min · 100 g^{-1} [32–34], and the measured arterial (A) and interstitial (I) concentrations. Thereafter, the rate of regional glucose uptake (rGU_{MD}) was calculated by multiplying glucose extraction by blood flow:

$$rGU_{MD} = [A\text{-}I] \times [1\text{-}e^{-PS/Flow}] \times Flow \quad 1$$

Calculation of lumped constant (LC). Lumped constant (LC) was calculated by dividing [^{18}F]FDG uptake (rGU_{FDG}) measured using PET by the glucose uptake measured using microdialysis (rGU_{MD}),

$$LC = rGU_{FDG}/rGU_{MD} = K_i \times [Glc]_p/rGU_{MD} \quad 2$$

Measurement of skeletal muscle glucose uptake with [^{18}F]FDG. To measure [^{18}F]FDG uptake in the skeletal muscle, the femoral region was moved into the gantry after completion of the abdominal scan. A dynamic scan for 20 min was carried out (6 · 180 s) and arterial blood sampling and measuring of plasma radioactivity was continued. Plasma and tissue time-activity curves for the anteromedial muscle compartments were analysed graphically to measure K_i [21]. Muscle glucose uptake was calculated by multiplying K_i by the plasma glucose concentration and dividing this by the LC value of 1.2 [12].

Whole body glucose uptake. Whole body glucose uptake as the glucose disposal rate was determined using the euglycaemic hyperinsulinaemic clamp technique, as previously described [22]. During hyperinsulinaemia, normoglycaemia was maintained using a variable infusion rate of 20 % glucose based on arterial plasma glucose determinations. The rate of whole body glucose uptake was calculated during the same time period that the measurements of adipose tissue blood flow and glucose uptake were made.

Other measurements. Arterial and plasma glucose was determined in duplicate by the glucose oxidase method (Analox GM9 Analyzer, Analox Instruments, London, UK). Serum insulin concentrations were measured basally and at 30-min intervals during insulin infusion using a double-antibody radioimmunoassay (Phadeseph Insulin RIA kit, Pharmacia and Upjohn, Uppsala, Sweden) with a detection limit of 2.5 mU/l.

Table 1. The characteristics of the study subjects. Values are means ± SEM

	Non-obese	Obese	*p*
n	7	7	
Age (years)	29 ± 2	32 ± 2	ns
BMI (kg/m^2)	23.6 ± 0.6	31.0 ± 1.0	< 0.001
Waist-to-hip-ratio	0.98 ± 0.01	1.06 ± 0.01	< 0.001
Fasting P-glucose (mmol/l)	5.5 ± 0.2	5.1 ± 0.2	ns
Fasting S-insulin (mU/l)	5.0 ± 0.8	9.9 ± 1.5	< 0.01

Statistical analyses. Results are expressed as means ± SEM. Statistical calculations were done using the SAS statistical programme package (SAS Institute, Cary, N. C., USA). Differences between the two groups were compared using Student's *t* test. Pearson's correlation coefficients were calculated where appropriate. A two-tailed *p*-value of less than 0.05 was regarded to be statistically significant.

Results

Metabolic characteristics during the studies. Characteristics of the study subjects are shown in Table 1. Fasting plasma glucose concentrations were similar in the non-obese and the obese subjects whereas fasting insulin concentrations were higher in the obese than in the non-obese subjects ($p < 0.01$; Table 1). During hyperinsulinaemia, interstitial glucose concentrations were similar in both groups (Table 2) and plasma glucose concentrations averaged 5.1 ± 0.1 mmol/l in both groups with coefficients of variation of 4.6 ± 1.9 % in the non-obese and 4.1 ± 1.7 % in the obese subjects. During hyperinsulinaemia, serum insulin concentrations were higher in the obese than in the non-obese subjects (81 ± 5 vs 62 ± 3 mU/L, $p < 0.05$, respectively).

Whole body and skeletal muscle glucose uptake. Insulin-stimulated whole body glucose uptake was 52 % lower in the obese than in the non-obese subjects ($p < 0.01$; Table 2.). Regression coefficient for the slopes of fractional rate of [^{18}F]FDG in skeletal muscle were excellent in all subjects ($r = 0.994 \pm 0.002$, $p < 0.01$ for all). Insulin-stimulated skeletal muscle glucose uptake measured using [^{18}F]FDG-PET was 59 % lower in the obese than in the non-obese subjects ($p < 0.01$; Table 2.).

Adipose tissue blood flow and [^{18}F]FDG uptake (rGU_{FDG}). Rates of insulin-stimulated adipose tissue blood flow measured with radiowater tended to be lower in the obese than in the non-obese subjects ($p = 0.06$; Table 2). When the fractional [^{18}F]FDG uptake was calculated using graphical analysis the points in the Patlak plot were stochastically scattered ($r = 0.978 \pm 0.004$, $p < 0.01$ for all; Fig. 3). During insulin stimulation fractional [^{18}F]FDG uptake values (K_i) in subcutaneous adipose tissue were higher in the non-obese than the obese subjects ($p < 0.05$, Table 2). Consequently, adipose tissue glucose uptake values measured using [^{18}F]FDG (rGU_{FDG}) and calculated by multiplying K_i by the plasma glucose concentration were higher in the non-obese than the obese subjects ($p < 0.05$; Table 2.). Adipose tissue glucose uptake values measured using [^{18}F]FDG (rGU_{FDG}) correlated with rates of insulin-stimulated adipose tissue blood flow in the pooled data ($r = 0.79$, $p < 0.01$) and with whole body glucose uptake values ($r = 0.77$, $p < 0.01$) in the pooled data (data not shown).

Adipose tissue glucose uptake measured using microdialysis (rGU_{MD}). Insulin-stimulated subcutaneous adipose tissue glucose uptake measured using microdialysis (rGU_{MD}) was higher in the non-obese than the obese subjects ($p < 0.05$; Table 2.) rGU_{MD} also correlated with whole body glucose uptake ($r = 0.61$, $p < 0.05$; data not shown). A correlation was observed between rGU_{FDG} and rGU_{MD} in the pooled data ($r = 0.82$, $p < 0.01$; data not shown).

Lumped constant and regional adipose tissue glucose uptake measured with PET (rGU_{PET}). The LC, calcu-

Table 2. Results of PET and microdialysis measurements

	Non-obese	Obese	All
Adipose tissue			
Blood flow (ml/kg · min^{-1})	33.4 ± 6.1	22.5 ± 2.4[a]	28.9 ± 2.4
Interstitial glucose (mmol/l)	4.0 ± 0.1	4.1 ± 0.1	4.0 ± 0.1
K_i (min^{-1})	0.0029 ± 0.0006	0.0015 ± 0.0002[b]	0.0022 ± 0.0003
rGU_{FDG} (μmol/kg · min^{-1})	14.9 ± 2.9	7.3 ± 0.8[b]	11.1 ± 1.8
rGU_{MD} (μmol/kg · min^{-1})	11.8 ± 1.7	7.6 ± 0.8[b]	9.7 ± 1.1
LC	1.26 ± 0.15	1.01 ± 0.15	1.14 ± 0.11
rGU_{PET} (μmol/kg · min^{-1})	11.9 ± 2.8	6.1 ± 0.8[b]	9.0 ± 1.6
Whole body			
Glucose disposal rate (μmol/kg · min^{-1})	42.7 ± 5.0	17.9 ± 3.2[c]	30.3 ± 4.5
Skeletal muscle			
rGU_{PET} (μmol/kg muscle · min^{-1})	52.4 ± 5.5	21.3 ± 4.7[c]	36.9 ± 5.5

Values are means ± SEM.
[a] $p = 0.06$
[b] $p < 0.05$
[c] $p < 0.01$ for obese vs non-obese subjects

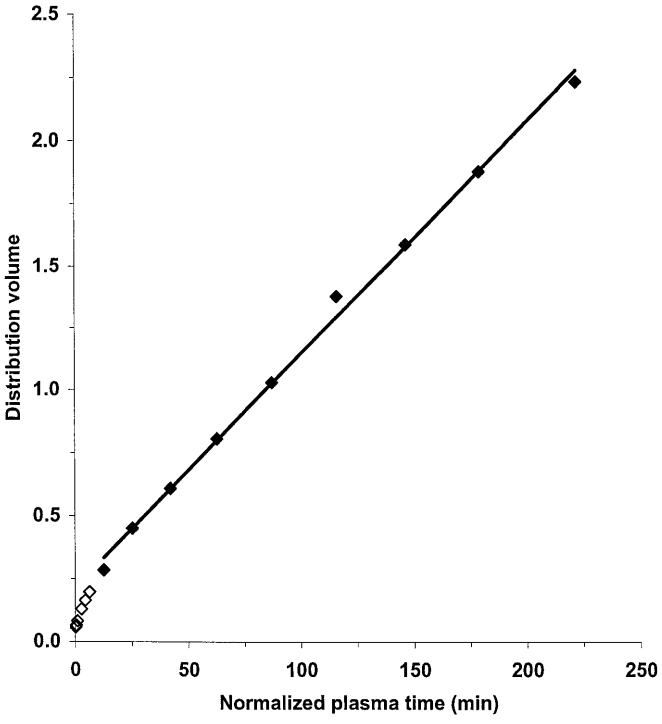

Fig. 3. An example of graphical analysis (Patlak plot) of subcutaneous adipose tissue in a non-obese subject. Fractional [^{18}F]FDG uptake increases linearly indicating metabolic trapping

lated by dividing rGU_{FDG} by rGU_{MD}, averaged 1.14 ± 0.11 for the entire group; 1.26 ± 0.15 for the non-obese and 1.01 ± 0.15 for the obese subjects (p = NS; Table 2). The range within the calculated LC-values was 0.78–1.70 in the non-obese and 0.68–1.67 in the obese subjects. No association was found between the LC and whole body glucose uptake values or between the LC and serum insulin concentrations. When regional PET derived glucose uptake (rGU_{PET}) was calculated by dividing rGU_{FDG} by the LC 1.14, non-obese subjects exhibited remarkably higher rates of rGU_{PET} than obese subjects ($p < 0.05$; Table 2.).

Discussion

Our study was undertaken to estimate the LC for [^{18}F]FDG in human adipose tissue during insulin stimulation and to measure adipose tissue glucose uptake using [^{18}F]FDG-PET. We found that the LC for [^{18}F]FDG averaged 1.14. Furthermore, we observed that insulin-stimulated glucose uptake was lower in subcutaneous adipose tissue in obese subjects than in non-obese subjects and that glucose uptake in skeletal muscle was considerably higher than in adipose tissue.

The LC value for [^{18}F]FDG has not been previously determined in human adipose tissue. The LC value of 1.14 is rather similar to that measured recently in human skeletal muscle (LC = 1.2) in studies in which the LC was measured using [^{18}F]FDG-PET and microdialysis, [12] or using [^{18}F]FDG-PET and A-V-differences [35] or the method based on triple-tracer and 2-deoxy-[^{14}C]glucose [36]. In this study, the LC for [^{18}F]FDG in adipose tissue was not found to change in insulin resistant obese subjects which is in accordance with our earlier skeletal muscle results [12].

The half-life of 109 min of [^{18}F]FDG enables scanning procedures extending over hours thus facilitating kinetic studies. Because [^{18}F]FDG is phosphorylated by hexokinase and trapped in the tissue, it is regarded as an ideal glucose tracer for PET studies in human myocardium and skeletal muscle [18, 19]. In this study, steady state conditions required by the model were attained by the insulin clamp technique. The [^{18}F]FDG was used in tracer amounts and tissue time-activity curves showed linear slopes (Fig. 3) supporting the assumption that [^{18}F]FDG was irreversibly trapped within adipocytes and not dephoshorylated.

In this study we used microdialysis independently of [^{18}F]FDG-PET to measure the interstitial glucose concentration in abdominal subcutaneous adipose tissue. The interstitial glucose concentrations measured were similar to those found in previous studies [8, 11]. All microdialysis catheters were calibrated in steady-state conditions using the internal reference technique, which has been previously shown to give similar recovery coefficients to the equilibration technique in human beings [23].

Investigators have evaluated the reliability of microdialysis technique for the assessment of adipose tissue glucose uptake in dogs [37]. They found that the mean calculated and measured venous plasma glucose concentrations were identical in adipose tissue, but glucose uptake rates measured using microdialysis and ^{133}Xenon washout techniques and Fick's principle only tended to correlate. However, it should be noted that a correlation is not to be expected if the range of the values evaluated is narrow. Moreover, any small errors in absolute values of fasting plasma glucose or in rates of blood flow assessed using the ^{133}Xenon washout technique influence glucose uptake rates [37]. Using a different experimental design, we found a correlation between glucose uptake measured using [^{18}F]FDG-PET and microdialysis ($r = 0.82$, $p < 0.01$). This study was done during steady-state hyperinsulinaemia and after an overnight fast. Furthermore, adipose tissue flow was measured directly with radiowater in the vicinity of the microdialysis probe in the same region of interest where the rates of glucose uptake and [^{18}F]FDG uptake were measured. Regions of interest were carefully drawn in the subcutaneous adipose tissue on the MR images and then copied onto the PET images. Thus, regional

glucose uptakes were calculated in the same region with two different and independent methods and from these measurements the LC was estimated.

Use of [^{15}O]H_2O and PET allows direct and regional assessment of perfusion without interference from other tissues and without invasive catheterisations. This method has been validated using plethysmography and used in skeletal muscle [29]. When applied to adipose tissue, the lower water content of adipose tissue (15 %) compared with muscle (79 %) was taken into account [30]. Error analysis of the autoradiographic method at low blood flow rates had been previously done [29].

In obese compared to non-obese subjects, glucose uptake in subcutaneous adipose tissue, measured with either microdialysis or [^{18}F]FDG-PET, was lower during insulin stimulation. Furthermore, skeletal muscle glucose uptake measured with [^{18}F]FDG-PET was significantly lower in the same subjects (Table 2). This is in contrast to previous reports [38] showing similar rates of glucose uptake per adipose tissue weight in lean and obese subjects after a meal but resistance to insulin stimulation of glucose uptake in the forearm muscle of obese subjects. It should be noted, however, that the data from the two studies might not be readily comparable because glucose concentration is not at steady state after a meal and, thus, could affect insulin independent glucose uptake. Also, it has been recently found that glucose uptake in subcutaneous adipose tissue was lower in obese subjects after a prolonged period of fasting [39].

The limitations of both microdialysis and [^{18}F]FDG-PET methods should be considered when interpreting these results. After appropriate calibration microdialysis permits reproducible and precise measurements of the glucose concentration in the interstitial fluid [8]. When the interstitial glucose concentration is used to determine glucose uptake from the interstitial space, the regional blood flow has to be known. In this study we used the combination of blood flow measurements with [^{15}O]H_2O-PET and interstitial glucose concentration measurements with microdialysis at the same time. To avoid disturbance from the extracellular space nearby the probe the first measurements were done 45 min after probe invention [8]. Measurement of adipose tissue and muscle glucose uptake using [^{18}F]FDG-PET and Patlak graphical analysis can be used reliably only under steady state conditions. Therefore the studies were carried out during steady state hyperinsulinaemic euglycaemia. For this reason, these results cannot be strictly compared with those after fasting or after a meal. Choice of ROIs has a crucial role in the determination of glucose uptake in the region. Therefore, the use of MRI as reference to PET is an almost obligatory tool for the anatomical mapping of adipose tissue and the reliable blood flow and glucose uptake rates.

Our adipose tissue blood flow results (mean 2.8 ml/100g · min^{-1}) are comparable with those measured recently in human subjects [10, 11, 40]. As expected, adipose tissue blood flow tended to be one third lower in the obese compared with non-obese subjects but there was no statistical significance between the different groups due to the limited number of subjects. Reduced adipose tissue blood flow rates in obese subjects have been reported [10, 41, 42]. The thicker layer of subcutaneous adipose tissue in obese subjects compared with non-obese subjects could partly explain the lower rates of adipose tissue blood flow [43].

Finally, it should be noted that regional differences exist as to the glucose uptake in subcutaneous adipose tissue, especially because the uptake rate in abdominal fat cells is more active in this regard than femoral adipocytes [44]. This, and the impact of an expanded fat cell mass in the obese subjects imply that our results might not be applied and generalized to the total body fat glucose uptake. To explore further the importance of the present results for the total body glucose uptake in insulin resistant obese subjects' measurements should be carried out in different adipose tissue regions.

In summary, [^{18}F]FDG-PET is a tool to investigate adipose tissue glucose metabolism in humans. Direct measurements with [^{18}F]FDG-PET and microdialysis suggest a LC value of 1.14 for [^{18}F]FDG in human subcutaneous adipose tissue during insulin stimulation and the LC does not appear to be altered in insulin-resistant obese subjects. The obese subjects showed resistance to insulin-stimulated glucose uptake in both subcutaneous adipose tissue and skeletal muscle.

Acknowledgements. This study was supported by grants from the Academy of Finland, Finnish Diabetes Foundation, Novo Nordisk Fund and Swedish Research Council (project number: T10864), Swedish Diabetes Association, Nordisk Research Fund (Nordisk Forskningsfond), Svenska Novo Research Fund (Svenska Novo Forskningsfond) and, Inga-Britt and Arne Lundbergs Foundation (Inga-Britt and Arne Lundbergs Stiftelse).

References

1. Colberg SR, Simoneau JA, Thaete FL, Kelley DE (1995) Skeletal muscle utilization of free fatty acids in women with visceral obesity. J Clin Invest 95: 1846–1853
2. Despres JP, Nadeau A, Tremblay A et al. (1989) Role of deep abdominal fat in the association between regional adipose tissue distribution and glucose tolerance in obese women. Diabetes 38: 304–309
3. Ross R, Fortier L, Hudson R (1996) Separate associations between visceral and subcutaneous adipose tissue distribution, insulin and glucose levels in obese women. Diabetes Care 19: 1404–1411
4. Kelley DE, Thaete FL, Troost F, Huwe T, Goodpaster BH (2000) Subdivisions of subcutaneous abdominal adipose

tissue and insulin resistance. Am J Physiol Endocrinol Metab 278: E941-E948
5. Abate N, Garg A, Peshock RM, Stray-Gundersen J, Adams-Huet B, Grundy SM (1996) Relationship of generalized and regional adiposity to insulin sensitivity in men with NIDDM. Diabetes 45: 1684–1693
6. Goodpaster BH, Thaete FL, Simoneau JA, Kelley DE (1997) Subcutaneous abdominal fat and thigh muscle composition predict insulin sensitivity independently of visceral fat. Diabetes 46: 1579–1585
7. Frayn KN, Coppack SW, Humphreys SM, Whyte PL (1989) Metabolic characteristics of human adipose tissue in vivo. Clin Sci (Colch) 76: 509–516
8. Lönnroth P, Jansson PA, Smith U (1987) A microdialysis method allowing characterization of intercellular water space in humans. Am J Physiol 253: E228-E231
9. Bolinder J, Hagström E, Ungerstedt U, Arner P (1989) Microdialysis of subcutaneous adipose tissue in vivo for continuous glucose monitoring in man. Scand J Clin Lab Invest 49: 465–474
10. Jansson PA, Larsson A, Smith U, Lönnroth P (1992) Glycerol production in subcutaneous adipose tissue in lean and obese humans. J Clin Invest 89: 1610–1617
11. Stallknecht B, Larsen JJ, Mikines KJ, Simonsen L, Bülow J, Galbo H (2000) Effect of training on insulin sensitivity of glucose uptake and lipolysis in human adipose tissue. Am J Physiol Endocrinol Metab 279: E376-E385
12. Peltoniemi P, Lönnroth P, Laine H et al. (2000) Lumped constant for [^{18}F]fluorodeoxyglucose in skeletal muscles of obese and nonobese humans. Am J Physiol Endocrinol Metab 279: E1122-E1130
13. Kolehmainen M, Ohisalo JJ, Kaartinen JM et al. (2000) Concordance of in vivo microdialysis and in vitro techniques in the studies of adipose tissue metabolism. Int J Obes Relat Metab Disord 24: 1426–32
14. Rosdahl H, Lind L, Millgård J, Lithell H, Ungerstedt U, Henriksson J (1998) Effect of physiological hyperinsulinemia on blood flow and interstitial glucose concentration in human skeletal muscle and adipose tissue studied by microdialysis. Diabetes 47: 1296–1301
15. Lönnroth P (1997) Microdialysis in adipose tissue and skeletal muscle. Horm Metab Res 29: 344–346
16. Phelps ME, Hoffman EJ, Selin C et al. (1978) Investigation of [^{18}F]2-fluoro-2-deoxyglucose for the measure of myocardial glucose metabolism. J Nucl Med 19: 1311–1319
17. Gambhir SS, Schwaiger M, Huang SC et al. (1989) Simple noninvasive quantification method for measuring myocardial glucose utilization in humans employing positron emission tomography and fluorine-18 deoxyglucose. J Nucl Med 30: 359–366
18. Nuutila P, Koivisto VA, Knuuti J et al. (1992) Glucose-free fatty acid cycle operates in human heart and skeletal muscle in vivo. J Clin Invest 89: 1767–1774
19. Laine H, Yki-Järvinen H, Kirvelä O et al. (1998) Insulin resistance of glucose uptake in skeletal muscle cannot be ameliorated by enhancing endothelium-dependent blood flow in obesity. J Clin Invest 101: 1156–1162
20. Phelps ME, Huang SC, Hoffman EJ, Selin C, Sokoloff L, Kuhl DE (1979) Tomographic measurement of local cerebral glucose metabolic rate in humans with (F-18)2-fluoro-2-deoxy-D-glucose: validation of method. Ann Neurol 6: 371–388
21. Patlak CS, Blasberg RG (1985) Graphical evaluation of blood-to-brain transfer constants from multiple-time uptake data. Generalizations. J Cereb Blood Flow Metab 5: 584–590
22. DeFronzo RA, Tobin JD, Andres R (1979) Glucose clamp technique: a method for quantifying insulin secretion and resistance. Am J Physiol 237: E214-E223
23. Lönnroth P, Strindberg L (1995) Validation of the 'internal reference technique' for calibrating microdialysis catheters in situ. Acta Physiol Scand 153: 375–380
24. Crouzel C, Clarc J, Brihaye C et al. (1993) Radiochemistry automation for PET. In: Stöcklin G, Pike V (eds) Radiopharmaceuticals for positron emission tomography. Dordrecht Academic Publisher Group, Kluwer, pp 45–90
25. Sipilä HT, Heselius S-J, Saarni HK, Ahlfors T (1985) A compact low-voltage ionization chamber for monitoring positron- and photon-emitters in flowing gases. Nucl Ins Meth Phys Res A238: 542–545
26. Hamacher K, Coenen HH, Stöcklin G (1986) Efficient stereospecific synthesis of no-carrier-added 2-[^{18}F]-fluoro-2-deoxy-D-glucose using aminopolyether supported nucleophilic substitution. J Nucl Med 27: 235–238
27. Alenius S, Ruotsalainen U (1997) Bayesian image reconstruction for emission tomography based on median root prior. Eur J Nucl Med 24: 258–265
28. Nuutila P, Raitakari M, Laine H et al. (1996) Role of blood flow in regulating insulin-stimulated glucose uptake in humans. Studies using bradykinin, [^{15}O]water, and [^{18}F]fluoro-deoxy-glucose and positron emission tomography. J Clin Invest 97: 1741–1747
29. Ruotsalainen U, Raitakari M, Nuutila P et al. (1997) Quantitative blood flow measurement of skeletal muscle using oxygen-15-water and PET. J Nucl Med 38: 314–319
30. Snyder WS, Cook MJ, Nasset ES, Karhausen LR, Parry Howells G, Tipton IH (1975) Report of the Task Group on Reference Man. International Commission on Radiological Protection, No 23, Pergamon Press, Oxford
31. Holmäng A, Muller M, Andersson OK, Lönnroth P (1998) Minimal influence of blood flow on interstitial glucose and lactate-normal and insulin-resistant muscle. Am J Physiol 274: E446-E452
32. Simonsen L, Bülow J, Madsen J (1994) Adipose tissue metabolism in humans determined by vein catheterization and microdialysis techniques. Am J Physiol 266: E357-E365
33. Linde B, Chisolm G, Rosell S (1974) The influence of sympathetic activity and histamine on the blood-tissue exchange of solutes in canine adipose tissue. Acta Physiol Scand 92: 145–155
34. Crone C, Levitt DG (1984) Capillary permeability to small solutes. In: Handbook of physiology. The cardivascular system. microcirculation. American Physiol Society, Bethesda pp.411–66
35. Kelley DE, Williams KV, Price JC, Goodpaster B (1999) Determination of the lumped constant for [^{18}F] fluorodeoxyglucose in human skeletal muscle. J Nucl Med 40: 1798–1804
36. Utriainen T, Lovisatti S, Mäkimattila S et al. (2000) Direct measurement of the lumped constant for 2-deoxy-[1-(14)C]glucose in vivo in human skeletal muscle. Am J Physiol Endocrinol Metab 279: E228-E233
37. Stallknecht B, Madsen J, Galbo H, Bülow J (1999) Evaluation of the microdialysis technique in the dog fat pad. Am J Physiol 276: E588-E595
38. Coppack SW, Fisher RM, Humphreys SM, Clark ML, Pointon JJ, Frayn KN (1996) Carbohydrate metabolism in insulin resistance: glucose uptake and lactate production by adipose and forearm tissues in vivo before and after a mixed meal. Clin Sci (Colch) 90: 409–415
39. Horowitz JF, Coppack SW, Klein S (2001) Whole-body and adipose tissue glucose metabolism in response to short-

term fasting in lean and obese women. Am J Clin Nutr 73: 517–522
40. Eriksson JW, Smith U, Waagstein F, Wysocki M, Jansson PA (1999) Glucose turnover and adipose tissue lipolysis are insulin-resistant in healthy relatives of type 2 diabetes patients: is cellular insulin resistance a secondary phenomenon? Diabetes 48: 1572–1578
41. Summers LK, Samra JS, Humphreys SM, Morris RJ, Frayn KN (1996) Subcutaneous abdominal adipose tissue blood flow: variation within and between subjects and relationship to obesity. Clin Sci (Colch) 91: 679–683
42. Bolinder J, Kerckhoffs DA, Moberg E, Hagström-Toft E, Arner P (2000) Rates of skeletal muscle and adipose tissue glycerol release in nonobese and obese subjects. diabetes 49: 797–802
43. Larsen OA, Lassen NA, Quaade F (1966) Blood flow through human adipose tissue determined with radioactive xenon. Acta Physiol Scand 66: 337–345
44. Mårin P, Rebuffe-Scrive M, Smith U, Björntorp P (1987) Glucose uptake in human adipose tissue. Metabolism 36: 1154–1160